AIP | Physics of Fluids

Interactions between active particles and dynamical structures in chaotic flow

Nidhi Khurana and Nicholas T. Ouellette

Citation: Phys. Fluids **24**, 091902 (2012); doi: 10.1063/1.4754873
View online: http://dx.doi.org/10.1063/1.4754873
View Table of Contents: http://pof.aip.org/resource/1/PHFLE6/v24/i9
Published by the AIP Publishing LLC.

Additional information on Phys. Fluids

Journal Homepage: http://pof.aip.org/
Journal Information: http://pof.aip.org/about/about_the_journal
Top downloads: http://pof.aip.org/features/most_downloaded
Information for Authors: http://pof.aip.org/authors

ADVERTISEMENT

Downloaded 26 Aug 2013 to 134.106.81.21. This article is copyrighted as indicated in the abstract. Reuse of AIP content is subject to the terms at: http://pof.aip.org/about/rights_and_permissions

Interactions between active particles and dynamical structures in chaotic flow

Nidhi Khurana and Nicholas T. Ouellette[a)]
Department of Mechanical Engineering and Materials Science, Yale University, New Haven, Connecticut 06520, USA

(Received 10 April 2012; accepted 11 September 2012; published online 26 September 2012)

Using a simple model, we study the transport dynamics of active, swimming particles advected in a two-dimensional chaotic flow field. We work with self-propelled, point-like particles that are either spherical or ellipsoidal. Swimming is modeled as a combination of a fixed intrinsic speed and stochastic terms in both the translational and rotational equations of motion. We show that the addition of motility to the particles causes them to feel the dynamical structure of the flow field in a different way from fluid particles, with macroscopic effects on the particle transport. At low swimming speeds, transport is suppressed due to trapping on transport barriers in the flow; we show that this effect is enhanced when stochastic terms are added to the swimming model or when the particles are elongated. At higher speeds, we find that elongated swimmers tend be attracted to the stable manifolds of hyperbolic fixed points, leading to increased transport relative to swimming spheres. Our results may have significant implications for models of real swimming organisms in finite-Reynolds-number flows. © *2012 American Institute of Physics*. [http://dx.doi.org/10.1063/1.4754873]

I. INTRODUCTION

For decades, measurements of how material is advected by fluid flows have been central both to the design of practical, engineering systems and to the understanding and prediction of naturally occurring flows. Since fluid mechanics has played a central role in the development of nonlinear dynamics more broadly, transport also plays a key role in dynamical systems theory.

Recent years have seen significant interest in the transport of material that does not exactly follow the fluid but that instead has additional terms in its equations of motion. Often, these additional terms arise from purely passive, static effects such as density mismatches between the advected material and the carrier fluid[1,2] or nontrivial particle shape.[3,4] But in many cases the transported material may have its own internal dynamics. In this case, it is said to be active.[5] The dynamics of active materials may even feed back on the flow field and modify it, though they need not. Although activity can be due to chemical[6] or mechanical[7] effects, it is perhaps most frequently biological:[8] that is, the transported particles are alive and can swim.

Swimming organisms exist on many size scales, and therefore in many flow regimes. Each regime lends itself to a different set of questions. For single-celled organisms at the micro-scale, where the Reynolds number is low and flows are well modeled as Stokes flows, researchers have long studied the ways in which swimmers propel themselves.[8–11] Since in this regime hydrodynamic interactions are long range and strong, studies have also focused on the collective behavior that arises in suspensions of microorganisms.[12–14] For macroscopic organisms such as fish, researchers also study propulsion with the hope of creating efficient, biomimetic swimming machines.[15] Far less work, however, has focused on the intermediate size regime, where the organisms are large enough that the flow can have nontrivial dynamics but the swimmers are weak enough that their intrinsic speed is small compared with the external flow. It is on this regime that we focus.

[a)]Electronic mail: nicholas.ouellette@yale.edu.

 © 2012 American Institute of Physics

Downloaded 26 Aug 2013 to 134.106.81.21. This article is copyrighted as indicated in the abstract. Reuse of AIP content is subject to the terms at: http://pof.aip.org/about/rights_and_permissions

The combination of swimming and complex flow fields has been shown to lead to qualitatively new behavior. For particles that are gyrotactic and can feel non-negligible gravitational torque, for example, swimming can lead to the accumulation of swimmers onto thin structures[16,17] in shear flows. Even in steady flows, gyrotaxis and swimming can produce a wide array of patterns.[18] In chaotic flows, it has been shown that swimming particles tend to accumulate in the chaotic regions as their speed increases.[19] We recently showed, however, that swimmers can also become trapped for very long times near the boundaries between chaotic and regular flow regions, with consequences for their long-time transport.[20]

Here, we build on our previous work by taking into account the nontrivial shape of real swimming organisms.[21] We also extend our model to include stochastic motion in addition to deterministic swimming, in an attempt to model organisms more realistically. We find in all cases that the addition of intrinsic motility to the particles allows them to interact with structures in the flow field in ways that simple fluid elements cannot. For spherical particles, this interaction takes the form of trapping near Kolmogorov-Arnold-Moser (KAM) tori in the background flow field, as we found in our previous work,[20] which leads to a suppression of the long-time transport of swimmers relative to fluid elements. We find that this hydrodynamic trapping effect is robust to the addition of stochasticity in the swimming model, and is in fact enhanced by it. When we change the shape of the swimmers from spheres to ellipsoids, we find more complex behavior. For small swimming speeds, transport is reduced even more than it is for spheres: the traps near the KAM tori appear to become attractors. At higher speeds, however, the transport of ellipsoids is *enhanced* relative to spheres, an effect that is due to the attraction of the ellipsoids to the stable manifolds of the hyperbolic fixed points in the flow. Thus, we show that the dynamical structures in the flow field interact with particle motility in nontrivial ways, and should be considered in models of, for example, organism encounter rates.[22] We also suggest that the variation from strongly suppressed to strongly enhanced transport we find for ellipsoidal particles over a small range of swimming speeds may be a factor in the tendency of real organisms to be aspherical.

We begin below by describing the properties of the advecting flow field and the details of the swimmer model in Sec. II. In Sec. III, we present our results for spherical particles. We focus separately on the cases of deterministic swimming, random motion added to the translational equations of motion, and random motion added to the rotational equation of motion. Then, in Sec. IV, we describe our results for the case of elongated, ellipsoidal swimming particles. Finally, we summarize our results and draw conclusions in Sec. V.

II. MODEL

A. Flow field

We are interested in the behavior of swimming particles suspended in a background flow that has nontrivial dynamics. If the flow field is too complex, however, we lose the ability to understand the detailed origin of any effects we observe. Thus, we choose to advect our swimmers in an analytically specified flow field that has well studied dynamics rather than to simulate, for example, a fully developed turbulent flow. We use a two-dimensional oscillating cellular flow,[23] following previous work,[19,20] since the dynamics of fluid elements in it are well characterized and understood.[2,23–25] Although this flow is two-dimensional and therefore cannot strictly exist in the real world, many of the geophysical flows that carry swimming organisms can be modeled as quasi-two-dimensional due to stratification and rotational effects. Additionally, due to effects such as gyrotaxis, small marine organisms often self-organize into confined thin layers.[17] Thus, our results are likely not wholly unrelated to real flows.

The flow field is given by the streamfunction

$$\psi(x, y, t) = \frac{U}{k} \sin[k(x + B \sin \Omega t)] \sin ky, \tag{1}$$

where U sets the velocity scale and $1/k$ is the characteristic length scale. Ω controls the rate at which the flow field oscillates, and the oscillation amplitude is given by B. The components of the flow

Downloaded 26 Aug 2013 to 134.106.81.21. This article is copyrighted as indicated in the abstract. Reuse of AIP content is subject to the terms at: http://pof.aip.org/about/rights_and_permissions

FIG. 1. (a) Snapshot of one unit cell of the flow field at zero phase (that is, for t such that $\sin \Omega t = 0$). Arrows show the local fluid velocity, and the shading shows the vorticity. As time progresses, the flow field oscillates sinusoidally in the horizontal direction. (b) Poincare section (at zero phase) for a fluid element initially in the chaotic sea, for $B = 0.12$ and $\Omega = 6.28$. Only one quarter of the unit cell is shown (corresponding to the lower-left vortex in (a)); the rest of the unit cell is related by symmetry. The central empty region is a period-1 elliptic island; the surrounding empty regions are a period-3 island chain. (c) Finite-time Lyapunov exponent (FTLE) field at zero phase. Again, only one quarter of the unit cell is shown.

velocity are then given by $u_x = \partial\psi/\partial y$ and $u_y = -\partial\psi/\partial x$. Thus, the streamfunction ψ plays the role of a Hamiltonian for the two-dimensional fluid mechanics, with the spatial dimensions x and y acting as the conjugate position-momentum pair; all the formalism and results of Hamiltonian chaos are then applicable to this flow.

For the time-independent, autonomous case ($B = 0$), this system is integrable and the flow mixes poorly: fluid elements move on periodic, closed orbits within vortical cells. Once time dependence is introduced, however, the extra degree of freedom admits chaotic particle trajectories.[26,27] In this regime, the flow field consists of quasi-periodic elliptic islands separated by a chaotic sea. The boundaries of the elliptic islands are transport barriers (KAM tori) that are impenetrable for fluid elements. The parameters B and Ω control the detailed shape and character of the elliptic islands and chaotic sea.[20]

Here, we present results for $B = 0.12$ and $\Omega = 6.28$. As shown in Fig. 1, this choice of parameters leads to a large period-1 island in each cell surrounded by a smaller period-3 island chain. Other choices of B and Ω lead to dynamics that are different in detail but that are not qualitatively different.[20] In Fig. 1, we show the flow field itself, a Poincare section for fluid elements in the chaotic sea, and the finite-time Lyapunov exponent field for the flow. We calculate the finite-time Lyapunov exponents by computing the eigenvalues of the Cauchy–Green strain tensor for this flow, as described in Ref. 28.

B. Swimmers

We model the swimmers as noninteracting, point-like, neutrally buoyant ellipsoids.[19,20] Each swimmer has an intrinsic velocity vector $\mathbf{u}_s$ with a constant magnitude u_s that points along the long axis of the swimmer. Even though the background flow is not fully turbulent, we are well outside of the Stokes flow regime. Thus, we assume one-way coupling with the flow field $\mathbf{u}$, so that the swimmer feels the flow but does not modify it (unlike some other types of advected active matter). Although this approximation would be inappropriate in a Stokes flow, it is valid for neutrally buoyant point-like particles in a finite-Reynolds-number flow where the fluid inertia is non-negligible. Since we do not include hydrodynamic interactions or other Stokes-flow effects in our model, we are assuming that the Reynolds number of our flow is finite.

The swimmer's overall velocity is given by the vector sum of the background fluid velocity and its intrinsic swimming vector. The direction of the intrinsic vector $\mathbf{u}_s$ can change via coupling to the flow vorticity and rate of strain. We emphasize that we include no inertial effects[1] or gyrotaxis[18] in our model; our swimmers are very simple.

In addition to these deterministic effects, some of which we studied previously,[20] we now also add stochastic terms to the equations of motion in order to capture the randomness that is often found in the motion of small swimming organisms.[29,30] We model this stochasticity by adding Gaussian random noise to the equations of motion for the swimmer. Therefore, the swimmers evolve via the

Downloaded 26 Aug 2013 to 134.106.81.21. This article is copyrighted as indicated in the abstract. Reuse of AIP content is subject to the terms at: http://pof.aip.org/about/rights_and_permissions

stochastic equations

$$\begin{aligned}
\mathrm{d}x &= \left[\frac{\partial\psi}{\partial y} + v_s\cos\theta\right]\mathrm{d}t + \sigma_s \mathrm{d}W_x,\\
\mathrm{d}y &= \left[-\frac{\partial\psi}{\partial x} + v_s\sin\theta\right]\mathrm{d}t + \sigma_s \mathrm{d}W_y,\\
\mathrm{d}\theta &= \left\{\alpha\left[\frac{1}{2}\left(\frac{\partial^2\psi}{\partial y^2} - \frac{\partial^2\psi}{\partial x^2}\right)\cos 2\theta - \frac{\partial^2\psi}{\partial x\partial y}\sin 2\theta\right] - \frac{1}{2}\left(\frac{\partial^2\psi}{\partial x^2} + \frac{\partial^2\psi}{\partial y^2}\right)\right\}\mathrm{d}t + \sigma_r \mathrm{d}W_r.
\end{aligned} \tag{2}$$

Note that the rotational equation of motion is essentially Jeffery's equation[3] with an additional stochastic term. Here, we have nondimensionalized all lengths by $1/k$, velocities by U, and times by $1/(Uk)$, the characteristic flow scales. Thus, the nondimensional swimming velocity is given by $v_s = u_s/U$, the nondimensional strength of the lateral Gaussian noise by σ_s, and the nondimensional strength of the rotational Gaussian noise by σ_r. W_x, W_y, and W_r are Wiener processes, and θ is the angle between the direction of the intrinsic swimming vector $\mathbf{u}_s$ and the horizontal axis. α is the eccentricity of the ellipsoids (given by $\alpha = (\gamma^2 - 1)/(\gamma^2 + 1)$, where γ is the aspect ratio); when $\alpha = 0$, the swimmers are spherical, and when $\alpha = 1$, the swimmers have infinite aspect ratio. To study the swimmer dynamics, we integrate these equations numerically and analyze the resulting trajectories for many swimmers. We note that we do not impose periodic boundary conditions on the swimmer trajectories.

III. SPHERICAL PARTICLES

A. Deterministic swimming

Unlike fluid elements, the swimmers do not obey Hamiltonian equations of motion due to their intrinsic motility. Thus, they are not confined by the same transport barriers as fluid elements are, and can cross into or out of the elliptic islands in the background flow field. Previously, we considered the dynamics of deterministic, spherical swimmers,[20] with the noise terms in Eq. (2) set to zero. Here, we briefly summarize the results of our prior work before considering the effects of stochasticity on spherical swimmers; we consider the effect of aspherical shape in Sec. IV.

Since the swimmers can pass through the KAM tori bounding the elliptic islands, they may explore more of the flow domain than fluid elements can. How far the swimmers penetrate into the elliptic islands, however, is a function of their intrinsic speed v_s. Previously, we observed that, as one would expect, very fast swimmers (those with $v_s > 0.065$ for these flow parameters) can explore the whole flow domain with equal probability: when the swimmers are fast enough, the effects of the background flow are relatively weak. Slower swimmers, however, behave differently. Although they can pass through the outer boundaries of the elliptic islands, they do not have enough motility to penetrate into the cores of the islands, and they enter the islands with low probability. But because entering and leaving the islands are symmetric processes, once they are in the islands they leave them only with low probability. These dynamics lead to the formation of "traps" in the flow field for swimmers.[20] These traps form just inside the elliptic islands of the background flow, and can confine swimmers for long times (thousands or tens of thousands of flow cycles) while they move on nearly bounded orbits.

The effect of these dynamical traps is clearly seen in the transport statistics of the swimmers. One might expect that adding motility to the particles should increase the rate at which they explore the flow domain. Due to the traps, however, we found that the particle transport can actually be *decreased* by adding motility, at least for small speeds. To quantify this effect, we studied the mean-squared displacement statistics for particles initially in the chaotic sea. At long times, fluid elements in this flow move diffusively;[23] that is, $\langle r^2\rangle = 4Dt$, where r is the distance from the initial position, D is a (chaotic) diffusion coefficient, and $\langle\cdot\rangle$ signifies an average taken over an ensemble of swimmers initially placed randomly in the chaotic sea. To measure D, we compute the displacement of this ensemble of swimmers from their initial positions as they evolve according to Eq. (2), and then fit the results to a linear power law. As shown in Fig. 2, the diffusion coefficients are suppressed relative

Downloaded 26 Aug 2013 to 134.106.81.21. This article is copyrighted as indicated in the abstract. Reuse of AIP content is subject to the terms at: http://pof.aip.org/about/rights_and_permissions

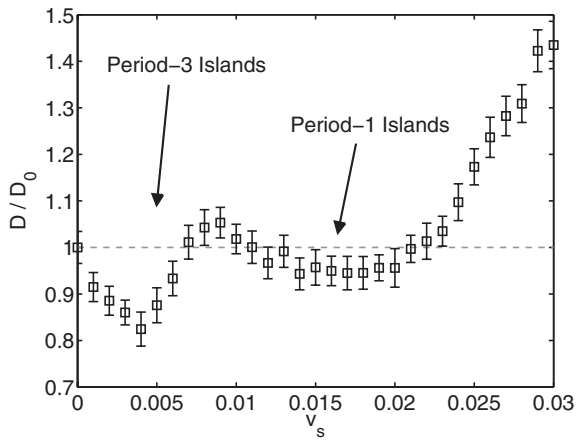

FIG. 2. Chaotic diffusion coefficient D normalized by D_0, the diffusion coefficient for fluid elements, as a function of the swimming speed v_s, for spherical swimmers with $\sigma_s = \sigma_r = 0$. Error bars are computed from the statistical fluctuations between many sets of simulations. Two distinct regions of suppressed long-time transport are seen, corresponding to trapping by the period-3 islands and by the period-1 islands.[20]

to D_0, the diffusion coefficient for fluid elements, for swimmers with small but finite swimming speeds. The effect is non-monotonic in v_s: as we showed previously, each type of elliptic island in the background flow has its own signature in the transport statistics.[20] The first local minimum in Fig. 2 corresponds to trapping in the period-3 islands, while the second (at higher v_s) is due to trapping in the larger period-1 islands. We note that despite this trapping behavior, we do not observe sub- or super-diffusive transients in the mean-squared displacement data.

B. Translational stochasticity

Having understood the effects of deterministic swimming in this system, we now introduce stochasticity. In order to separate the various possible effects, we first consider only translational stochasticity; that is, we choose $\sigma_s \neq 0$ in Eq. (2), but fix $\sigma_r = 0$ and $\alpha = 0$.

In Fig. 3, we show the chaotic diffusion coefficients for particles with $v_s = 0$ but with $\sigma_s \neq 0$. In addition to modeling randomly swimming organisms, this case captures the behavior of colloidal or other simple Brownian particles in the presence of a background advecting flow (though

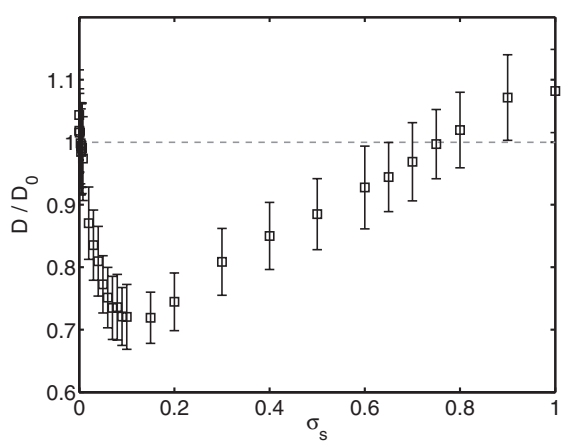

FIG. 3. Chaotic diffusion coefficient D normalized by D_0 as a function of σ_s, for $v_s = 0$, $\sigma_r = 0$, and $\alpha = 0$. When compared with Fig. 2, transport is more strongly suppressed, but the distinct signatures of each type of elliptic island are no longer present.

Downloaded 26 Aug 2013 to 134.106.81.21. This article is copyrighted as indicated in the abstract. Reuse of AIP content is subject to the terms at: http://pof.aip.org/about/rights_and_permissions

outside of the Stokes regime). Several features of the curve in Fig. 3 are noteworthy. First, strong stochasticity ($\sigma_s \gtrsim 1$) leads to enhanced transport coefficients. The physics of this result is clear: when the random motion along the particle trajectories is comparable in strength to the advective forcing, the particles must move more rapidly. But the suppressed chaotic diffusion coefficients seen in Fig. 2 are still present for $\sigma_s < 0.8$, and in fact are suppressed more strongly than they are for deterministic swimming. Additionally, the multiple local minima in the diffusivity curve in Fig. 2 that corresponded to the two types of elliptic islands in the background flow are now no longer present; rather, only a single minimum occurs in Fig. 3.

To understand this behavior, we consider again the mechanism leading to the transport suppression in the deterministic swimming case. As their intrinsic speed increases, the swimmers can begin to cross the KAM tori surrounding the elliptic islands. Since v_s remains small, however, they still move approximately as fluid elements. They, therefore, move on nearly bounded orbits inside the islands, and remain trapped there for long times. As v_s increases, the swimmers can penetrate further and further into the islands, and small islands confine them only weakly. This effect is the origin of the distinct signature of each type of elliptic island. For the parameters considered here, for example, swimmers with small v_s can penetrate into the (weaker) period-3 islands but not into the period-1 islands. They can therefore be trapped only by the period-3 islands. For higher v_s, the weak period-3 islands no longer influence their dynamics, but the period-1 islands play a much larger role since the swimmers can move deeper into them. Once v_s is high enough, the period-1 islands are also not strong enough to influence their dynamics, and the transport is enhanced.

When we introduce random motion for the swimmers rather than deterministic swimming, the picture changes. The swimmers can now wander deep into the strong period-1 islands even for relatively small values of σ_s, leading to a stronger, single feature in the transport statistics. To illustrate this effect, we show in Fig. 4 the average time to cross a flow cell boundary for the global minima in Figs. 2 and 3, namely a deterministic swimmer with $v_s = 0.004$ and a stochastic swimmer with $\sigma_s = 0.15$. More intense regions in Fig. 4 correspond to stronger traps: the more strongly confined a swimmer is, the longer it will take it to wander between flow cells. The cases of deterministic and stochastic swimming are clearly quite different. Even though the largest average trapping times are similar, the spatial distribution varies significantly. In the deterministic case (Fig. 4(a)), the swimmers can enter only a small region of the period-1 elliptic island around its periphery; when it does, however, it tends to remain there for a long time. The stochastic swimmer, on the other hand, can explore the entire flow domain, but its transport is strongly suppressed while it is inside the period-1 island. For values of v_s high enough for a deterministic swimmer to reach the centers of the period-1 islands (for $v_s \gtrsim 0.025$), the dynamics of the swimmers are different enough from those of fluid elements that the trapping is fairly weak, as can be seen in Fig. 2. Thus, the phenomenon of trapping is not only robust to noise along the swimmer trajectories but is in

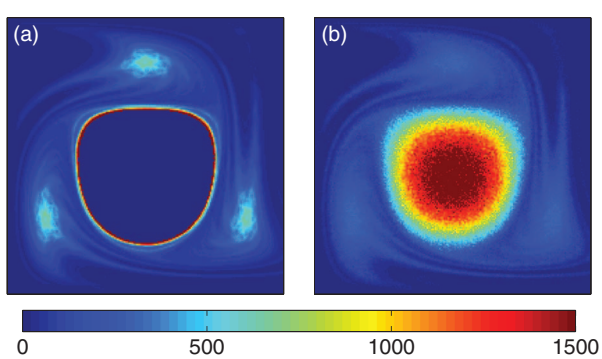

FIG. 4. Average time for a swimmer to cross a cell boundary as a function of its spatial location for (a) $v_s = 0.004$ and $\sigma_s = \sigma_r = 0$ and (b) $\sigma_s = 0.15$ and $v_s = \sigma_r = 0$. Only one quarter of the flow domain is shown. The shade/color bar gives the cell-crossing time in flow cycles. For the deterministic swimmer in (a), trapping is strong in the period-3 islands and on a small ring just inside the period-1 island. The purely stochastic swimmer can wander into the core of the period-1 island, where trapping is strongest.

Downloaded 26 Aug 2013 to 134.106.81.21. This article is copyrighted as indicated in the abstract. Reuse of AIP content is subject to the terms at: http://pof.aip.org/about/rights_and_permissions

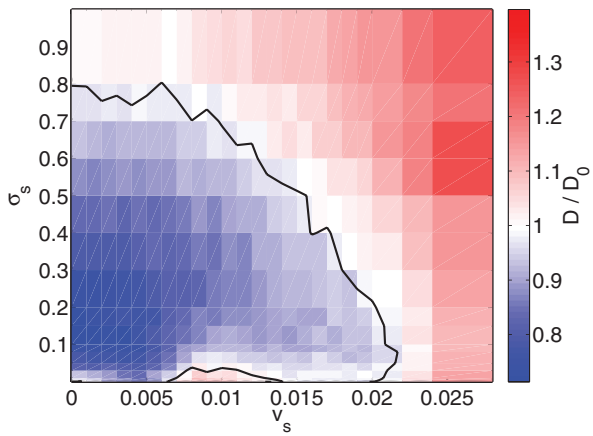

FIG. 5. Chaotic diffusion coefficients D in the two-dimensional parameter space spanned by v_s and σ_s for $\sigma_r = 0$. The shade/color bar shows D relative to D_0. The black line separates the regions of suppressed transport ($D/D_0 < 1$) from those of enhanced transport ($D/D_0 > 1$).

fact enhanced by it. Similar results have been found previously for chaotic scattering systems, and a similar mechanism was proposed.[31]

In order to better model real organisms, we now consider the case of both $v_s \neq 0$ and $\sigma_s \neq 0$: swimmers that combine deterministic and stochastic motion. In Fig. 5, we show the relative diffusion coefficient for such swimmers in the two-dimensional space spanned by v_s and σ_s. The basic features seen in Fig. 5 are similar to the two limiting cases we have already considered. There is a large region of parameter space in which transport is suppressed, although it will be enhanced if either v_s or σ_s is large enough. Additionally as the stochasticity in the system increases, the detailed dependence of transport suppression on the flow topology (with a separate signature for each elliptic island) disappears. This result suggests that the basic phenomenology of trapping and reduced transport that we observe in our idealized system is likely robust even in more realistic situations that include randomness.

C. Rotational stochasticity

Adding rotational rather than translational noise to the swimmers (that is, setting $\sigma_s = 0$ but $\sigma_r \neq 0$) changes the picture dramatically. Now the stochasticity in the system only reorients the spherical swimmer without changing its position. For this reason, setting $\sigma_r \neq 0$ and $v_s = 0$ is identical to the case of a fluid element: reorienting a passive sphere changes nothing about its motion. When v_s is finite, however, rotational diffusion can change its motion significantly. Figure 6 shows the relative chaotic diffusion coefficients for the (σ_r, v_s) parameter space. In comparison with translational diffusion (Fig. 5), rotational diffusion suppresses transport for a much larger fraction of parameter space, and the strongest suppression occurs for high values of σ_r rather than low values, in contrast to σ_s.

This result is straightforward to understand. All that finite rotational noise can do is reorient the swimmer; as long as v_s remains small, the swimmer will still take small steps (relative to the imposed fluid advection). With large σ_r, however, these steps will be in essentially random directions. This limit is thus similar to the moderate-σ_s, low-v_s regime in Fig. 5. Physically, the transport suppression results from the ability of the rotationally diffusing swimmers to wander into the cores of the elliptic islands even for small v_s. To illustrate this effect, we show in Fig. 7 the average times to cross flow cell boundaries for $v_s = 0.004$ (the same case as shown in Fig. 4(a)) and four different values of σ_r. As σ_r increases, the swimmers wander deeper into the elliptic islands, and are trapped there for very long times.

Downloaded 26 Aug 2013 to 134.106.81.21. This article is copyrighted as indicated in the abstract. Reuse of AIP content is subject to the terms at: http://pof.aip.org/about/rights_and_permissions

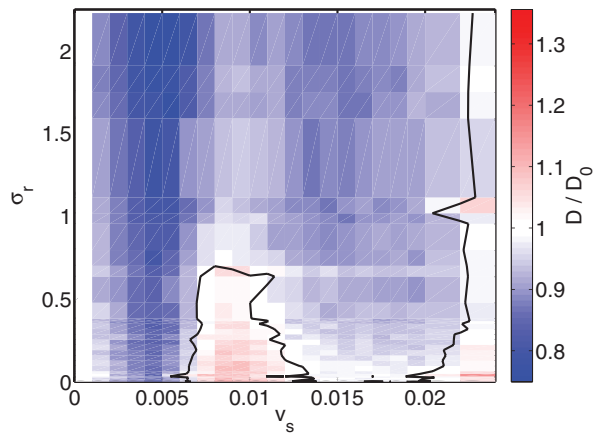

FIG. 6. Chaotic diffusion coefficients D in the two-dimensional parameter space spanned by v_s and σ_r for $\sigma_s = 0$. The shade/color bar shows D relative to D_0. The black line separates the regions of suppressed transport ($D/D_0 < 1$) from those of enhanced transport ($D/D_0 > 1$). Transport is suppressed in larger region of parameter space than it was for purely translational stochasticity case in Fig. 5.

IV. ELLIPSOIDAL PARTICLES

We have shown above that adding noise to the motion of the swimmers changes the details of the trapping but does not fundamentally alter their behavior. Changing their shape, however, is qualitatively different. We varied the shape of the swimmers by changing their eccentricity α from $\alpha = 0$ (spheres) to $\alpha = 1$ (infinite-aspect-ratio ellipsoids). As can be seen by studying Eq. (2), allowing α to be nonzero changes the nature of the problem. In addition to coupling the swimmer to the rate of strain in the flow field instead of just the vorticity, nonzero α also allows true attractors into the system, since the trace of the Jacobian J of the dynamical system is given by

$$\mathrm{Tr}(J) = -\alpha\left[\left(\frac{\partial^2\psi}{\partial y^2} - \frac{\partial^2\psi}{\partial x^2}\right)\sin 2\theta + 2\frac{\partial^2\psi}{\partial x\partial y}\cos 2\theta\right]. \tag{3}$$

Thus, for $\alpha \neq 0$, Liouville's theorem no longer applies to the system and the swimmers can aggregate.

This modification of the dynamical system leads to significant changes in the behavior of the swimmers. In general, we find that particle elongation enhances all of the interactions between the flow and the swimming: if the transport of a swimming sphere is suppressed relative to a fluid element, the transport of an ellipsoid will be suppressed more, while if the transport of a sphere is enhanced, the transport of an ellipsoid will be enhanced more. Thus, elongation tends to increase the sensitivity and response of the swimmer to its dynamical environment.

To illustrate these effects and to demonstrate the mechanisms that lead to the enhanced sensitivity, we show in Fig. 8 results for ellipsoidal swimmers at a low swimming speed of $v_s = 0.002$. At

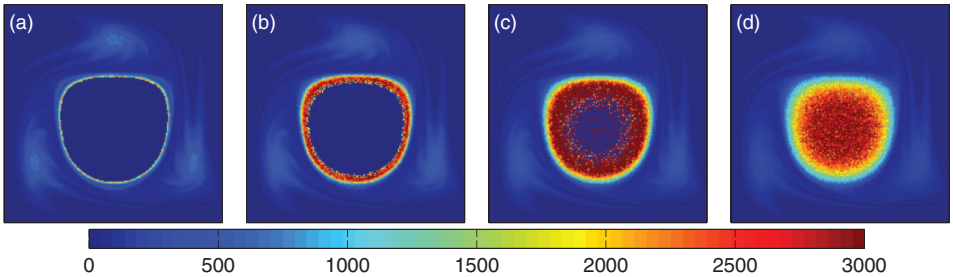

FIG. 7. Spatially resolved maps of the average time to cross a cell boundary for $v_s = 0.004$, and $\sigma_r =$ (a) 0.1, (b) 1.0, (c) 3.0, and (d) 6.0. $\sigma_s = 0$ for all panels. The shade/color bar gives the cell-crossing times in flow cycles. The times are much longer than the comparable $v_s = 0.004$, $\sigma_r = 0$ case shown in Fig. 4(a).

Downloaded 26 Aug 2013 to 134.106.81.21. This article is copyrighted as indicated in the abstract. Reuse of AIP content is subject to the terms at: http://pof.aip.org/about/rights_and_permissions

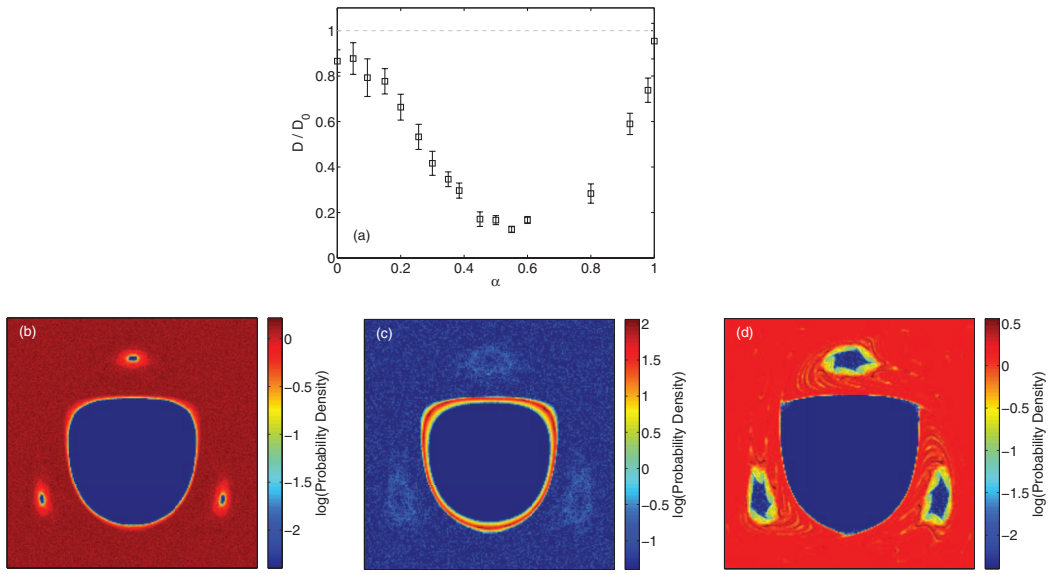

FIG. 8. (a) Chaotic diffusion coefficient D normalized by D_0 as a function of eccentricity α for deterministic swimmers with $v_s = 0.002$. Transport is much more strongly suppressed for ellipsoids of intermediate eccentricities than it is for spheres. (b)–(d) Probability density functions of swimmer position for (b) $\alpha = 0$, (c) $\alpha = 0.5$, and (d) $\alpha = 1$. The strong suppression of transport for ellipsoidal particles is due to the formation of attractors.

this value of v_s, spherical swimmers are primarily influenced by the period-3 islands in the flow, and their transport is suppressed relative to fluid elements. In Fig. 8(a), we show the chaotic diffusion coefficients for swimmers with $v_s = 0.002$ as a function of their eccentricity α. As α increases, the behavior changes wildly, and the chaotic diffusion coefficient can drop to less than 20% of the value for fluid elements. The maximum suppression of the transport occurs for $\alpha \approx 0.55$, corresponding to an aspect ratio of about 1.85. For larger eccentricities, the transport becomes faster again, approaching the value for fluid elements at $\alpha = 1$ (infinite aspect ratio).

To understand the mechanism behind this behavior, we show in Figs. 8(b)–8(d) the probability density functions (PDFs) of swimmer position (essentially the likelihood of finding a swimmer in a given location) for $\alpha = 0$, 0.5, and 1. We consider only swimmers with initial positions in the chaotic sea. As discussed above, spherical swimmers (Fig. 8(b)) tend to be in the chaotic sea, which they explore uniformly, but can also enter the periphery of the period-3 and period-1 islands. If they enter these islands, they remain stuck for long times, but the probability of entering the islands is low at this value of v_s. The situation is markedly different for $\alpha = 0.5$ (Fig. 8(c)). Now, the swimmers are highly likely to be found just inside the period-1 island. In fact, it appears that this region is an attractor for these ellipsoids: once a swimmer enters this region, it does not escape. The highly suppressed transport we see for this value of α is thus due to the formation of this attractor. For higher values of α, however, the attractor disappears, and the transport of highly elongated ellipsoids is similar to that of spheres. Nevertheless, as shown in Fig. 8(d), their spatial distribution is quite different. High-α ellipsoids do not enter the period-1 island at all (compare with the Poincare section for fluid elements show in Fig. 1(b)), and do not explore the chaotic sea uniformly. Instead, as described further below, these highly elongated particles interact strongly with the Lagrangian strain field, which is itself nonuniform.

In Fig. 9, we show the same quantities plotted in Fig. 8 but for a high speed of $v_s = 0.08$. At this speed, we expect the transport of the swimmers to be enhanced relative to fluid elements, and indeed, as shown in Fig. 9(a), the chaotic diffusion coefficient for spherical swimmers with $v_s = 0.08$ is more than 2.5 times higher than it is for fluid elements. But here again we find a strong dependence on swimmer shape: for ellipsoidal swimmers with $\alpha \gtrsim 0.3$, the chaotic diffusion coefficient is nearly 4 times higher than it is for fluid elements.

Downloaded 26 Aug 2013 to 134.106.81.21. This article is copyrighted as indicated in the abstract. Reuse of AIP content is subject to the terms at: http://pof.aip.org/about/rights_and_permissions

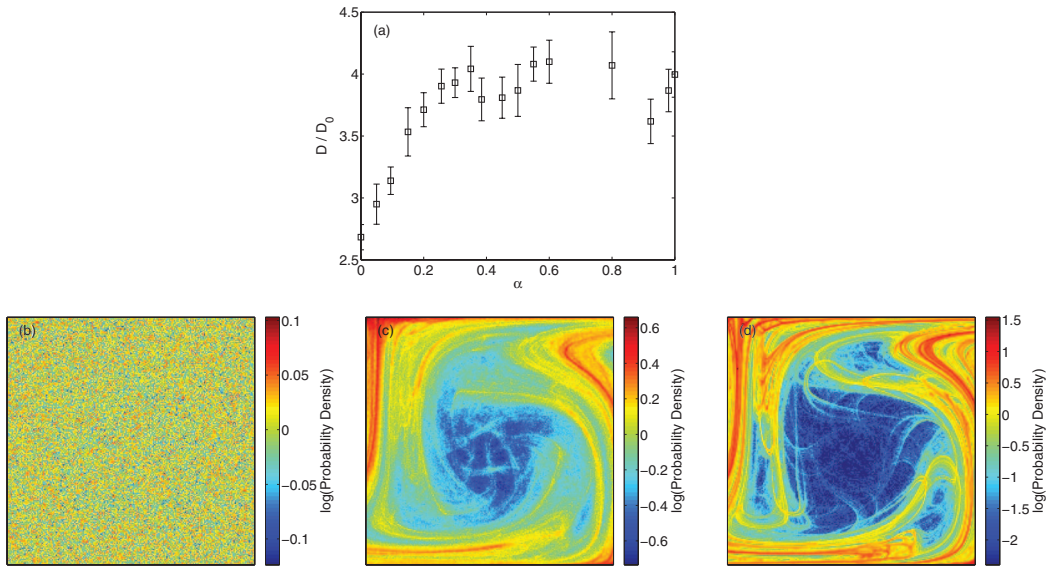

FIG. 9. (a) Chaotic diffusion coefficient D normalized by D_0 as a function of eccentricity α for deterministic swimmers with $v_s = 0.08$. For this speed, transport of ellipsoidal particles is strongly enhanced relative to spheres. (b)–(d) Probability density functions of swimmer position for (b) $\alpha = 0$, (c) $\alpha = 0.5$, and (d) $\alpha = 1$. The strong enhancement of transport is due to the clustering of ellipsoids on the stable manifolds of the hyperbolic fixed points.

To understand this result, we turn again to PDFs of the swimmer positions, shown in Fig. 9 for $\alpha = 0, 0.5$, and 1. At $v_s = 0.08$, spherical particles explore the entire flow domain with roughly equal probability, as shown in Fig. 9(b). But the situation is very different for higher eccentricities. For $\alpha \gtrsim 0.3$, the PDFs of swimmer position begin to develop detailed spatial structure, which becomes very strong as $\alpha \to 1$. Comparing Fig. 9(d) with Fig. 1(c), we see that the structures picked out by elongated swimmers coincide with regions where the Lyapunov exponent is large, which themselves map out the stable manifolds of the hyperbolic points in the flow.[32] This behavior is somewhat reminiscent of passive ellipsoids in chaotic flows, which show alignment with the manifolds;[4] here, however, the swimmers not only align with the manifolds but also aggregate on them. The attraction of elongated swimmers to the stable manifolds also explains why their transport is enhanced relative to spherical particles even though the spheres explore more of the flow domain, since the stable manifolds are some of the fastest-moving regions in the flow.

The existence of attractors in the dynamics for ellipsoidal particles has strong implications for the rate at which swimmers encounter one another. To demonstrate this effect, we fix the number density of swimmers in our system (we use a population of 1000 swimmers in each quarter of the flow domain) and consider the average distance δ_{NN} between a swimmer and its nearest neighbor. In Fig. 10, we show δ_{NN}, scaled by the value for passive particles at the same number density, as a function of α for $v_s = 0.002$ and 0.08. The attractor seen in Fig. 8(c) is clearly evident in Fig. 10(a), and leads to swimmers that are much more likely to encounter each other. But Fig. 10(b) shows that encounter rates are also enhanced for elongated swimmers at high v_s even though their transport is also enhanced. Thus, more rapid transport of the swimmers does not necessarily lead to lower encounter rates, since the elongated swimmers still tend to accumulate on dynamical flow structures.

As a final note, we also considered the effects of adding stochastic terms to the equations of motion for the ellipsoids. The results are similar to those we found for spherical swimmers. Adding stochasticity to the rotational equation of motion does not change the swimmer behavior qualitatively. Translational stochasticity allows the swimmers to wander into the center of the elliptic islands even for small swimming speeds. It smooths out some of the more detailed signatures of the flow structures, and appears to shrink the basins of attraction for the attractors. The essence of the behavior we observe for the ellipsoids, however, remains the same.

Downloaded 26 Aug 2013 to 134.106.81.21. This article is copyrighted as indicated in the abstract. Reuse of AIP content is subject to the terms at: http://pof.aip.org/about/rights_and_permissions

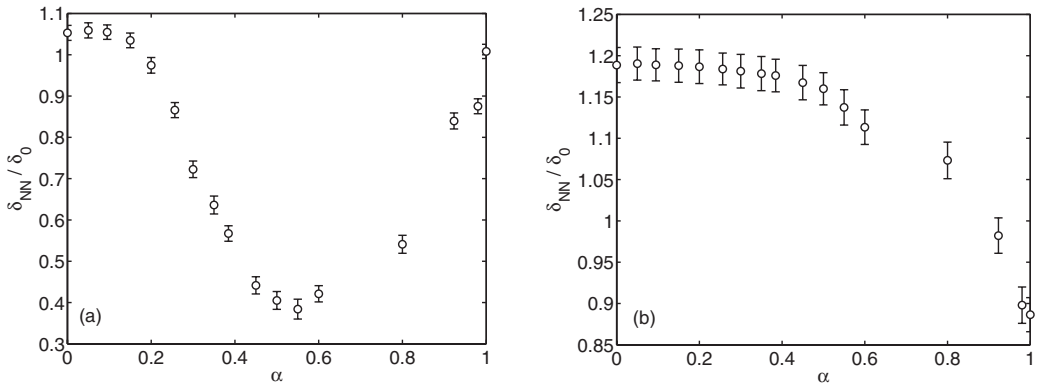

FIG. 10. Mean nearest neighbor distance δ_{NN} scaled by the value for passive particles δ_0 as a function of eccentricity for (a) $v_s = 0.002$ and (b) $v_s = 0.08$. High aspect ratio swimmers tend to be closer to each than spherical swimmers are, leading to enhanced encounter rates.

V. SUMMARY AND CONCLUSIONS

We have studied the dynamics of model swimming particles in a chaotic advecting flow field. By explicitly adding stochastic terms to the equations of motion for the swimmer, we have shown that not only are our previous results showing a suppression of long-time transport for small swimming speeds[20] robust to noise, but that they are in fact enhanced by it. We showed that both with and without stochasticity this suppression of transport is due to the interaction of the swimmers with dynamical structures (in this case transport barriers and non-mixing islands) in the flow field.

We also found that changing the shape of the swimmers leads to richer behavior and enhancement of the effects of the particle motility: when spherical swimmers show reduced transport, the transport of ellipsoidal swimmers is more strongly reduced, and when spherical swimmers move faster than passive particles, ellipsoidal swimmers move yet faster. Thus, for the same range of accessible swimming speeds, an elongated body shape allows a swimmer to respond more strongly to the flow field. Additionally, we showed that elongated swimmers tend to lie closer to their neighbors than spherical swimmers do due to their tendency to cluster on the dynamical flow structures. These effects may be a factor in explaining the observation that most real swimming organisms (zooplankton, for example) are not spherical.

[1] M. R. Maxey and J. J. Riley, "Equation of motion for a small rigid sphere in a nonuniform flow," Phys. Fluids **26**, 883 (1983).
[2] A. Babiano, J. H. E. Cartwright, O. Piro, and A. Provenzale, "Dynamics of a small neutrally buoyant sphere in a fluid and targeting in Hamiltonian systems," Phys. Rev. Lett. **84**, 5764 (2000).
[3] G. B. Jeffery, "The motion of ellipsoidal particles immersed in a viscous fluid," Proc. R. Soc. London, Ser. A **102**, 161 (1922).
[4] S. Parsa, J. S. Guasto, M. Kishore, N. T. Ouellette, and J. P. Gollub, "Rotation and alignment of rods in two-dimensional chaotic flow," Phys. Fluids **23**, 043302 (2011).
[5] Z. Toroczkai and T. Tél, "Introduction: Active chaotic flow," Chaos **12**, 372 (2002).
[6] J. R. Howse, R. A. L. Jones, A. J. Ryan, T. Gough, R. Vafabakhsh, and R. Golestanian, "Self-motile colloidal particles: From directed propulsion to random walk," Phys. Rev. Lett. **99**, 048102 (2007).
[7] R. Dreyfus, J. Baudry, M. L. Roper, M. Fermingier, H. A. Stone, and J. Bibette, "Microscopic artificial swimmers," Nature (London) **437**, 862 (2005).
[8] T. J. Pedley and J. O. Kessler, "Hydrodynamic phenomena in suspensions of swimming microorganisms," Annu. Rev. Fluid Mech. **24**, 313 (1992).
[9] M. J. Lighthill, "On the squirming motion of nearly spherical deformable bodies through liquids at very small Reynolds numbers," Commun. Pure Appl. Math. **5**, 109 (1952).
[10] E. M. Purcell, "Life at low Reynolds number," Am. J. Phys. **45**, 3 (1977).
[11] E. Lauga and T. R. Powers, "The hydrodynamics of swimming microorganisms," Rep. Prog. Phys. **72**, 096601 (2009).
[12] X.-L. Wu and A. Libchaber, "Particle diffusion in a quasi-two-dimensional bacterial bath," Phys. Rev. Lett. **84**, 3017 (2000).
[13] P. T. Underhill, J. P. Hernandez-Ortiz, and M. D. Graham, "Diffusion and spatial correlations in suspensions of swimming particles," Phys. Rev. Lett. **100**, 248101 (2008).

Downloaded 26 Aug 2013 to 134.106.81.21. This article is copyrighted as indicated in the abstract. Reuse of AIP content is subject to the terms at: http://pof.aip.org/about/rights_and_permissions

[14] D. Saintillan and M. Shelley, "Instabilities, pattern formation, and mixing in active suspensions," Phys. Fluids **20**, 123304 (2008).
[15] J. E. Colgate and K. M. Lynch, "Mechanics and control of swimming: a review," IEEE J. Ocean. Eng. **29**, 660 (2004).
[16] J. O. Kessler, "Hydrodynamic focusing of motile algal cells," Nature (London) **313**, 218 (1985).
[17] W. M. Durham, J. O. Kessler, and R. Stocker, "Disruption of vertical motility by shear triggers formation of thin phytoplankton layers," Science **323**, 1067 (2009).
[18] W. M. Durham, E. Climent, and R. Stocker, "Gyrotaxis in a steady vortical flow," Phys. Rev. Lett. **106**, 238102 (2011).
[19] C. Torney and Z. Neufeld, "Transport and aggregation of self-propelled particles in fluid flows," Phys. Rev. Lett. **99**, 078101 (2007).
[20] N. Khurana, J. Blawzdziewicz, and N. T. Ouellette, "Reduced transport of swimming particles in chaotic flow due to hydrodynamic trapping," Phys. Rev. Lett. **106**, 198104 (2011).
[21] Marcos, J. R. Seymour, M. Luhar, W. M. Durham, J. G. Mitchell, A. Macke, and R. Stocker, "Microbial alignment in flow changes ocean light climate," Proc. Natl. Acad. Sci. U.S.A. **108**, 3860 (2011).
[22] F. G. Schmitt and L. Seuront, "Intermittent turbulence and copepod dynamics: Increase in encounter rates through preferential concentration," J. Mar. Syst. **70**, 263 (2008).
[23] T. H. Solomon and J. P. Gollub, "Chaotic particle transport in time-dependent Rayleigh-Bénard convection," Phys. Rev. A **38**, 6280 (1988).
[24] T. Nishikawa, Z. Toroczkai, and C. Grebogi, "Advective coalescence in chaotic flows," Phys. Rev. Lett. **87**, 038301 (2001).
[25] R. Festa, A. Mazzino, and M. Todini, "Dynamics of light particles in oscillating cellular flows," Phys. Rev. E **80**, 035301 (2009).
[26] H. Aref, "Stirring by chaotic advection," J. Fluid Mech. **143**, 1 (1984).
[27] J. M. Ottino, *The Kinematics of Mixing: Stretching, Chaos, and Transport* (Cambridge University Press, Cambridge, 1989).
[28] G. A. Voth, G. Haller, and J. P. Gollub, "Experimental measurements of stretching fields in fluid mixing," Phys. Rev. Lett. **88**, 254501 (2002).
[29] H. C. Berg and D. A. Brown, "Chemotaxis in Escherichia coli analysed by three-dimensional tracking," Nature (London) **239**, 500 (1972).
[30] M. Polin, I. Tuval, K. Drescher, J. P. Gollub, and R. E. Goldstein, "Chlamydomonas swims with two "gears" in a Eukaryotic version of run-and-tumble locomotion," Science **325**, 487 (2009).
[31] E. G. Altmann and A. Endler, "Noise-enhanced trapping in chaotic scattering," Phys. Rev. Lett. **105**, 244102 (2010).
[32] G. Haller, "Distinguished material surfaces and coherent structures in three-dimensional fluid flows," Physica D **149**, 248 (2001).

Downloaded 26 Aug 2013 to 134.106.81.21. This article is copyrighted as indicated in the abstract. Reuse of AIP content is subject to the terms at: http://pof.aip.org/about/rights_and_permissions